Dispersion Characterization in Layered Double Hydroxide/Nylon 66 Nanocomposites Using FIB Imaging

Y. D. Zhu,[1] G. C. Allen,[1] J. M. Adams,[2] D. Gittins,[3] M. Herrero,[4] P. Benito,[4] P. J. Heard[1]

[1]Interface Analysis Center, University of Bristol, Bristol BS2 8BS, United Kingdom
[2]School of Engineering and Computer Science, University of Exeter, Exeter EX4 4QF, United Kingdom
[3]Performance Minerals and Pigments, Central R&D, IMERYS Minerals Ltd., Par Moor Center, St. Austell, PL24 2SQ, United Kingdom
[4]Departamento de Química Inorgánica, Universidad de Salamanca, 37008 Salamanca, Spain

ABSTRACT: Layered double hydroxides (LDHs), a newly emerging 2D host material, consist of cationic brucite-like layers and exchangeable interlayer anions. In this work, the morphology and dispersion of LDH particles in LDH/Nylon 66 (salt) nanocomposites has been investigated using focused ion beam (FIB) techniques, transmission electron microscopy (TEM) and X-ray diffraction (XRD). The FIB images show that LDHs are present in the polymer phase dispersed to different degrees, with partial intercalation, exfoliation, and aggregation all being observed. The most even dispersion was achieved in nanocomposites with the lowest loading (0.5 wt % LDH). Residual tactoids and agglomerates were most common in the samples made with the highest concentration of LDHs studied here (5 wt %). The dispersion observed using FIB was consistent with TEM and XRD analysis, yet this technique had significant benefits in terms of time and simplicity over these ''conventional'' technologies. © 2008 Wiley Periodicals, Inc. J Appl Polym Sci 108: 4108–4113, 2008

Key words: Nylon 66; LDH; nanocomposite; dispersion; FIB

INTRODUCTION

Since the Toyota Research Group carried out the initial work to produce Nylon 6/clay nanocomposites,[1,2] the use of polymeric nanocomposites in various engineering applications has become state-of-the-art because these materials have high potential for delivering very significant property improvements while adding only small amounts of nanoparticles to polymer matrices. These improvements include modulus, strength, heat resistance, and reductions of gas permeability and flammability,[3–5] all of which can be achieved with little increase in weight, significant in many applications in vehicle transports for example.

As an alternative to the natural layered silicate clay (montmorillonite) commonly used for the preparation of polymeric nanocomposites, a new class of nanocomposites employs synthetic nanoparticles, layered double hydroxides (LDHs), with opposite charge to montmorillonite, i.e., the layers are cationic rather than anionic. Nanocomposites based on LDHs have recently generated interest from researchers due to their special properties in a wide range of application such as catalysis, adsorption, structural applications, and drug delivery.[6,7] LDHs have positively charged hydroxide layers and interlayers containing exchangeable anions and water molecules. Compositions can be expressed as: $[M^{2+}_{1-x}M^{3+}_{x}(OH)_2]_{intra}[A^{m-}_{x/m}\cdot nH_2O]_{inter}$, where M^{2+} and M^{3+} are metal ions, A is the anion, and intra and inter denote the intralayer domain and the interlayer space, respectively. LDH layers consist of edge-sharing octahedra; each of the octahedra having a central cation coordinated with six hydroxyl groups. The layers are 0.48–0.49 nm thick[8,9] and their planar dimensions can be tuned by properly adjusting the synthesis conditions. The most important features of LDHs are their large variety of compositions and the tunable layer charge density.[10]

It has been commonly agreed that particle dispersion plays an important role in the improvement of mechanical and other properties in nanocomposites, because a high degree of dispersion ensures maximum interface area and the maximum impact on polymer crystallinity and structure. Generally, the dispersion of particles in the polymer matrix is characterized by scanning electron microscopy (SEM), transmission electron microscopy (TEM) and X-ray diffraction (XRD).[11–14] SEM can give a general

description of particle dispersion while TEM allows a qualitative understanding of the internal structure, spatial distribution of the various phases, and visualization of the intercalation and exfoliation of platelet stacks. The shape, position, and intensity of the basal peaks in XRD may provide quantitative information on intercalated clay structures. However, each of these techniques has drawbacks. SEM is not the perfect method for characterization of nanocomposites, because it is difficult to obtain meaningful data from an unprepared surface. Traditional TEM sample preparation, involving mechanical milling and ion gun sputtering, is often time-consuming and requires experience. Moreover, this preparation technique is not suitable for composites containing a mixture of soft and hard materials. XRD, although it offers a convenient method for determining the interlayer spacing in the original layered clay and in the intercalated nanocomposites, can say little about the spatial distribution of the layers or any structural nonhomogeneities. Focused ion beam (FIB) techniques, however, seem to have considerable potential benefits, which arise from the unique microsectioning capability and acceptable resolution. FIB polishing gives a very good surface for this type of measurement.

In this study, FIB imaging has been used to observe the dispersion of LDHs in Nylon 66 matrix. TEM and XRD are used to verify the FIB results.

EXPERIMENTAL

Preparation of LDH/Nylon 66 nanocomposites

Raw materials, $Mg(NO_3)_2 \cdot 6H_2O$, $Al(NO_3) \cdot 9H_2O$, adipic acid and hexamethylene diamine were obtained from Panreac (Spain). First, the parent Mg-Al LDH was prepared by pH controlled coprecipitation[15] and microwave-hydrothermal treatment. A solution of $Mg(NO_3)_2 \cdot 6H_2O$ and $Al(NO_3)_3 \cdot 9H_2O$ with a total Mg-Al concentration of 0.6 mol/L and a Mg:Al molar ratio of 2, was added drop-wise to 100 mL of deionized water (adipic acid) with intense stirring. The usage of adipic acid was twice the anionic exchange capacity of the LDHs (i.e., adipic acid/Al molar ratio = 2). The pH of the mixture was kept constant (~10 pH) by simultaneous addition of an aqueous solution containing 1 mol/L NaOH. The resulting slurry was aged by microwave-hydrotermal treatment for 3 h at 125°C as reported elsewhere.[16] The microwave-hydrothermal treatment was carried out in a Milestone Ethos Plus microwave oven with a teflon-coated autoclave.

The LDH/Nylon 66 nanocomposites were prepared by *in situ* intercalative polymerization. A given amount of hexamethylene diamine and adipic acid with molar ratio of 1 was added to 50 mL of LDH slurry. The mixture was refluxed under nitro-

gen for 3 h at 100°C after the water was removed and dried under vacuum. Several mixtures with different LDH concentrations (0, 0.5, 1, and 5 wt %) were prepared. All mixtures were divided into two parts. One part was a Nylon 66 salt nanocomposite, while the other part was polymerized at 190°C for 200 min in an inert atmosphere to obtain LDH/Nylon 66 nanocomposites.

Characterization

The morphology and dispersibility of LDH in the Nylon 66 matrix were characterized by means of FIB, TEM, and XRD.

A FEI FIB201 was used for sectioning, high-resolution imaging, and also for TEM sample preparation. The instrument was capable of producing a gallium ion beam of between 7 (at 1 pA beam current) and 300 nm (at 12 nA) in diameter at 30 keV energy.

TEM samples were prepared by FIB.[17] A thin section was polished from both sides until it was ~100-nm thick. The polished section was cut away using the ion beam, and then the entire sample was removed from the FIB system to an *ex-situ* lift-out workstation comprising an optical microscope and micromanipulator. The slice was extracted and placed onto a grid for TEM microscopy. TEM image was obtained using a JEOL 1200EX with an accelerating voltage of 100 kV.

A Siemens D-500 diffractometer with Cu Kα_1 radiation (λ = 1.54050 Å) at a generator voltage of 40 kV and a current of 30 mA was used to study the diffraction behavior of the Nylon 66 (salt)/LDHs nanocomposites. All the experiments were conducted in the reflection mode at ambient temperature between 1° and 10° 2θ. The scanning step size was 0.05°.

RESULTS AND DISCUSSION

The FIB images for the neat Nylon 66 (salt) and the nanocomposites containing 0.5, 1, and 5 wt % LDHs are shown in Figures 1 and 2. It is very obvious that there are voids in the FIB images of the Nylon 66 salt and its nanocomposites prepared without heat treatment, while an ordered, wrinkle-like structure is visible in the FIB images of Nylon 66 and its nanocomposites, which had been heat treated.

The voids may be caused by the volatilization of components of Nylon salt, such as hexamethylene diamine. During the polycondenzation, the inert gas will also accelerate the volatilization process, thus forming more voids. At high temperature, these void defects in crystals of Nylon 66 salt may cause the large molecules to nucleate, resulting in successive and epitaxial crystallization processes.[18,19] The wrinkles visible on the FIB images may relate to this crystallization effect in the polymer phase, and
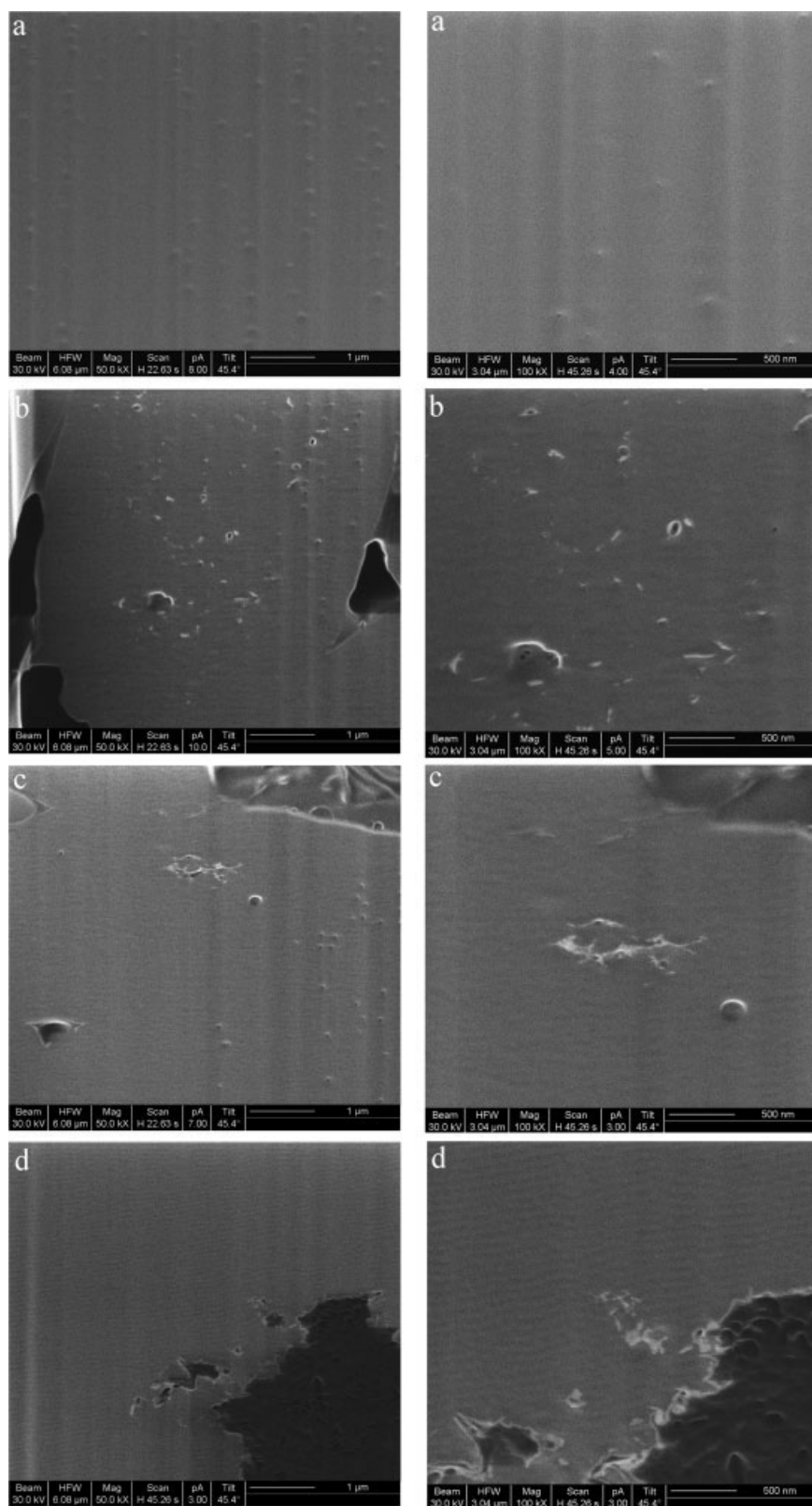
Figure 1 FIB images of neat Nylon 66 salt and its nanocomposites at different LDH loadings without thermal treatment. (a) Neat Nylon 66 salt, (b) 0.5 wt % LDH, (c)1 wt % LDH, and (d) 5 wt % LDH (left: low magnification, right: high magnification).
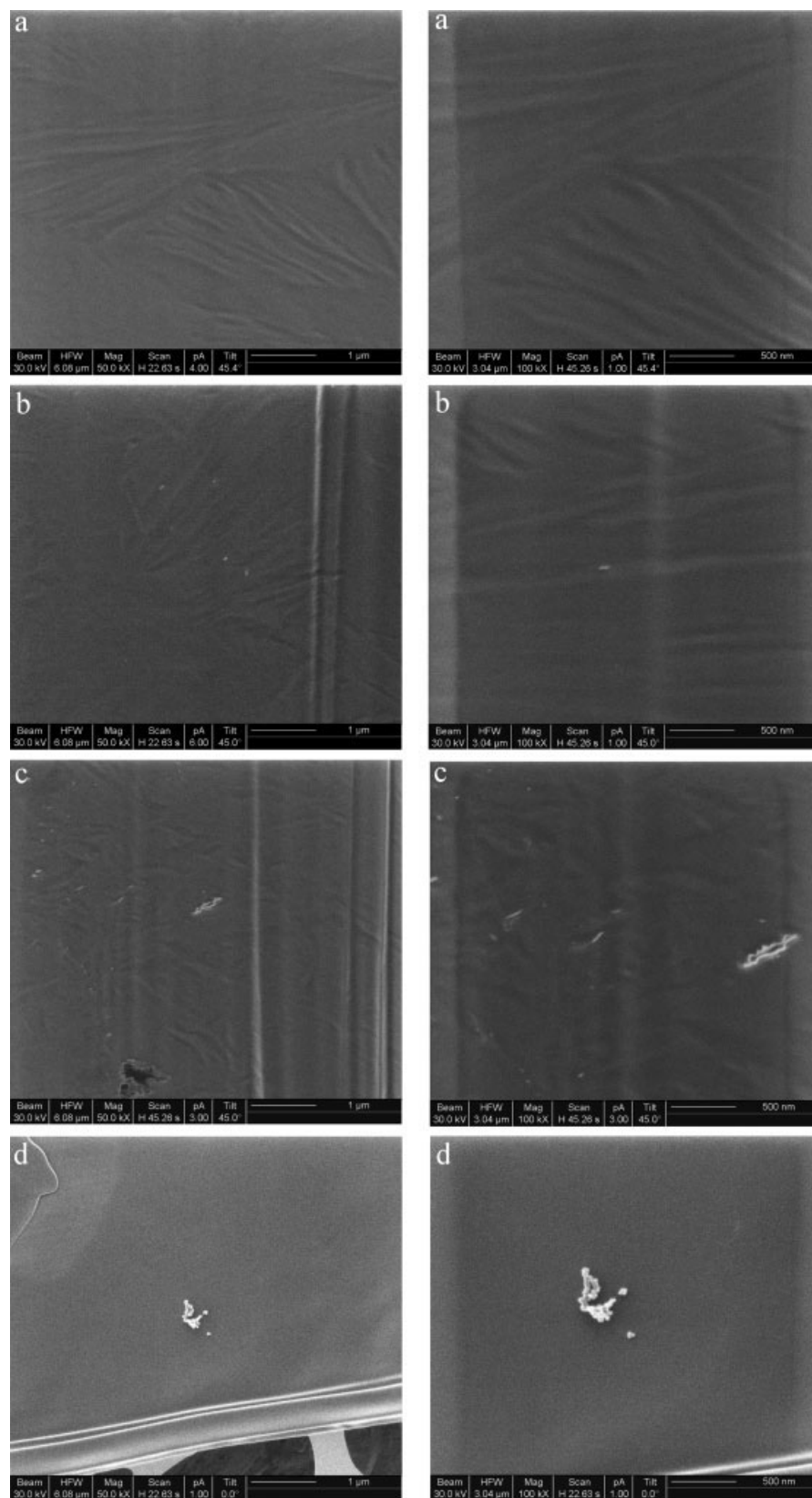
Figure 2 FIB images of neat Nylon 66 and its nanocomposites at different LDH loadings with thermal treatment. (a) Neat Nylon 66, (b) 0.5 wt % LDH, (c) 1 wt % LDH, and (d) 5 wt % LDH (left: low magnification, right: high magnification).
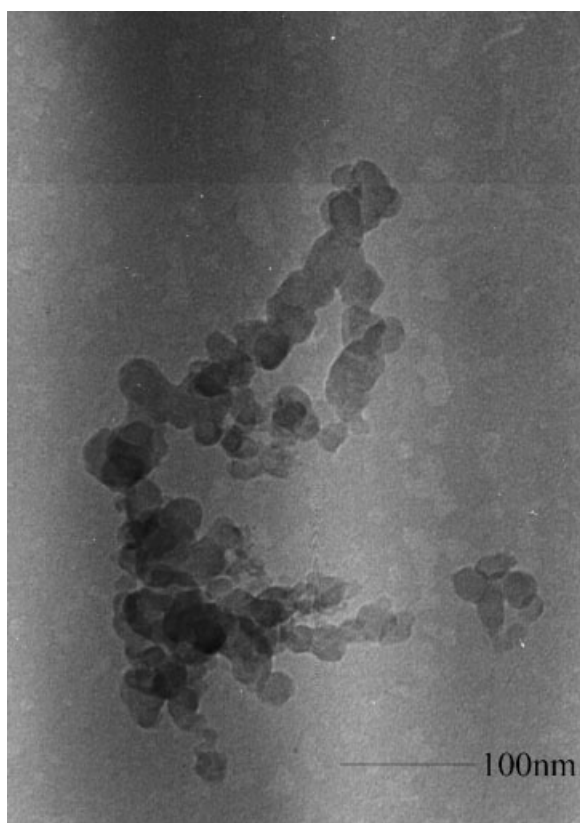
Figure 3 TEM image of LDH/Nylon 66 nanocomposites with 5 wt % LDH loading.

future experiments will be conducted to investigate this phenomenon using optical techniques.

The FIB images of nanocomposites [Figs. 1(b–d) and 2(b–d)] show a set of particles of different sizes dispersed in a nonregular way in the organic phase. The micrographs indicate the presence of reasonably well-dispersed small features, which may be intercalated layers or exfoliated tactoids of LDH crystals. The tactoids are mostly in the form of thin platelets having a thickness in the range 11–40 nm and a length in the range 27–110 nm. When the LDHs are modified with the carboxyl anion, the basal spacing is ~1.3 nm (XRD test). The length of the typical hexagon of LDH on the edge of an agglomerate is between 70 and 200 nm.[20] On the basis of the basal spacing and the measured thickness range, the number of platelets estimated is around 8–30, which means that the LDHs are partially intercalated and mesoscale tactoids exist. At the same time, the planar plate size of length (27–110 nm) is considerably lower than that of the raw material (27–200 nm). This indicates that layer breakage occurs during compounding.

However, larger particles are also observed, which may be aggregates caused by the residual tactoids that have not been sufficiently well dispersed. Tactoids with length over 140 nm are observed in the

FIB images. The ''large particles/aggregates'' are especially obvious (and probably especially serious) in the nanocomposites with the higher LDHs concentrations. Furthermore, a few small agglomerates of LDH layers with variable thickness also appear in the nanocomposite with 1.0 and 5.0 wt % LDH loadings. Generally, the distribution of the LDH particles throughout the matrix appears to be inhomogeneous.

Note also that the heat treatment does not seem to have a significant impact on the dispersion of LDHs in the Nylon 66 matrix.

A TEM specimen taken from the Nylon 66/LDH nanocomposites with 5 wt % LDH loading prepared using FIB is shown in Figure 3. Compared with the FIB image from the same specimen (Fig. 2d), TEM clearly offers much higher spatial resolution than FIB imaging. However, this study demonstrates that FIB imaging also proves to be a simple and reliable method for the assessment of particle dispersion at the nanometer scale. It should be noted that it takes more than 3 h for the preparation and imaging of the TEM specimen while just half an hour is needed for the preparation of FIB specimen and imaging.

To provide further evidence to support the FIB results, XRD was also carried out. The XRD patterns of the modified LDHs, neat Nylon 66, and representative samples of Nylon 66 (salt)/LDH nanocomposites are shown in Figure 4. The basal spacing of modified LDHs is about 1.3 nm ($2\theta = 6.5°$), which is
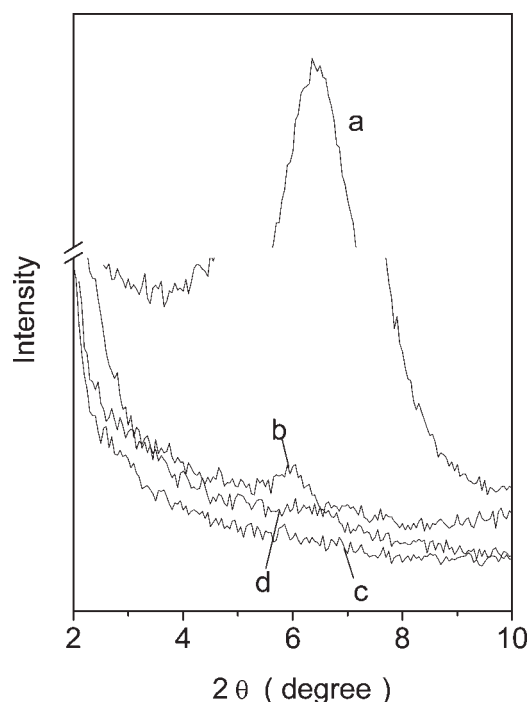

Figure 4 XRD of (a) modified LDH, (b) LDH/Nylon salt (5 wt % LDH), (c) LDH/Nylon 66 salt (0.5 wt % LDH), and (d) LDH/Nylon 66 (0.5 wt % LDH).

similar to the reported value of LDHs intercalated with adipate.[21] For the nanocomposite samples, the basal peak (001) at $2\theta = 6.5°$ shifts to lower angle or disappears with the decreasing loading of LDHs, indicating complete exfoliation of the LDH layers.[14] At 5 wt % LDH loading, the presence of the shoulder ($2\theta = 6.0°$) indicates a mixed nano/micro structure. That is, the LDH layers have been partially exfoliated and partially intercalated into the matrix, while some residual tactoids still exist. On the other hand, at 0.5 wt % LDH loading, the diffraction peak disappears, leaving a broad diffraction background, an indication of exfoliation. Apparently, the particle dispersion in the nanocomposites is better at low LDH concentrations than that at higher ones. These observations and related results support the findings from FIB and TEM analysis.

CONCLUSIONS

To summarize, the dispersion of LDHs in Nylon 66 may be qualitatively estimated from analysis of FIB images. FIB images show that the LDHs are present in the polymer phase dispersed to different degrees. The small features that are visible may consist of intercalated and exfoliated layers. The larger features are undoubtedly aggregates or agglomerates. The best dispersion is achieved in Nylon 66 (salt)/LDH nanocomposites with the lowest loading (0.5 wt % LDH). Residual tactoids and agglomerates are most commonly found in the samples made with the highest concentrations of LDH (5 wt %). These dispersion results observed using FIB also are consistent with information derived from TEM and XRD.

Although TEM imaging can, in principle, provide higher resolution, FIB imaging is found to provide a quicker and reliable solution for observing meso-scale-macroscopic (close-nano) particle dispersion in nanocomposites. Further comparison between TEM and FIB imaging for the characterization of other types of nanocomposites is currently being carried out.

References

1. Fukushima, Y.; Okada, A.; Kawasumi, M.; Kurauchiand, T.; Kamigaito, O. Clay Miner 1988, 23, 27.
2. Usuki, A.; Kojima, Y.; Kawasumi, M.; Okada, A.; Fukushima, Y.; Kurauchiand, T.; Kamigaito, O. J Mater Res 1993, 8, 1179.
3. Chen, L.; Wong, S. C.; Liu, T. X.; Lu, H. X.; He, C. B.; J Polym Sci 2004, 42, 2759.
4. Friedrich, K.; Fakirovand, S.; Zhang, Z. Polymer Composites: From Nano- to Macro-scale; Springer: New York, 2005.
5. Gain, O.; Espuche, E.; Pollet, E.; Alexandreand, M.; Dubois, P. H. J Polym Sci 2005, 43, 205.
6. Rives, V. Layered Double Hydroxides: Present and Future; Nova Science Publishers: New York, 2001.
7. Xu, Z. P.; Stevenson, G.; Lu, C. Q.; Lu G. Q. J Phys Chem B 2006, 110, 16923.
8. Meyn, M.; Beneke, K.; Lagaly, G. Inorg Chem 1990, 29, 5201.
9. Borja, M.; Dutta, P. K. J Phys Chem 1992, 96, 5434.
10. De Roy, A.; Forano, C.; EL Malkiand, K.; Besse, J. P. In Synthesis of Microporous Materials; Occelli, M. L.; Robson, H. E., Eds.; Van Nostrand Reinhold: New York, 1992, p 108.
11. Wagener, R.; Reisinger, T. J. G. Polymer 2003, 44, 7513.
12. Jordan, J.; Jacob, K. I.; Tannenbaum, R.; Sharaf, M. A.; Jasiuk, I. Mater Sci Eng A Struct 2005, 393, 1.
13. Zhao, J.; Morgan A. B.; Harris, J. D. Polymer 2005, 46, 8641.
14. Rothon, R. N. Particulate-filled polymer composites; Rapra Technology Limited: Shropshire, UK, 2003.
15. Reichle, W. T. Solid State Ionics 1986, 22, 135.
16. Benito, P.; Labajos, F. M.; Rocha, J.; Rives, V. Microporous Mesoporous Mater 2006, 94, 148.
17. Heard, P. J.; Preston, J. S.; Parsons, D. J.; Coxand, J.; Allen, G. C. Colloid Surf A 2004, 244, 67.
18. Macchi, E. M.; Orosoff, N. M.; Morawetz, H. J Polym Sci Part A-1: Polym Chem 1968, 6 2033.
19. Zeng, H. M.; Feng, L. Polym Commun 1983, 5, 321.
20. Zammarano, M.; Bellayer, S. V.; Gilman, J. W.; Francesch, M.; Beyer, F. L.; Harris, R. H.; Meriani, S. Polymer 2006, 47, 652.
21. Anbarasan, R.; Lee, W. D.; Im, S. S. Bull Mater Sci 2005, 28, 145.